

A NEW DISTANCE ESTIMATOR AND SPATIAL DISTRIBUTION OF GRBS OBSERVED BY BATSE

Heon-Young Chang¹, Suk-Jin Yoon², and Chul-Sung Choi³

¹ *Korea Institute for Advanced Study*

207-43 Cheongryangri-dong Dongdaemun-gu, Seoul 130-012, Korea,

² *Center for Space Astrophysics and Department of Astronomy, Yonsei University*

134 Shinchon-dong Seodaemun-gu, Seoul 120-749, Korea

³ *Korea Astronomy Observatory*

36-1 Hwaam-dong, Yusong-gu, Taejon 305-348, Korea

`hyc@ns.kias.re.kr, sjyoon@csa.yonsei.ac.kr, cschoi@kao.re.kr`

ABSTRACT

We propose a redshift estimator for the long ($T_{90} > 20$) gamma-ray bursts (GRBs) observed by the BATSE. It is based on an empirical relation between the redshift and the power-law index of power density spectra (PDSs) of the observed GRBs. This relation is constructed by using the fact that the power-law index is dependent upon a characteristic timescale of GRB light curves which are inevitably stretched by cosmological time dilation. We construct the empirical relation using both individual PDSs and averaged PDSs. An error estimates of z are 1.09 and 1.11 for the empirical relation by individual PDS fits, 1.72 and 1.56 by averaged PDS fits, for the least squares fit and the maximum likelihood fit, respectively. We attempt to determine the spatial distribution of the GRBs observed by the BATSE as a function of redshifts on the basis of the resulting redshift estimator. We find that the obtained spatial distribution of the observed GRBs seems consistent with that of the GRBs whose redshifts are reported, even though the estimated errors are not very accurate. The GRBs observed by the BATSE seem distributed within $z \sim 5 - 6$. This result has implications on theoretical calculations of stellar formations at high redshifts and beaming geometry via a statistical study of the observed GRBs involving beaming-induced luminosity functions. We discuss such implications, and possible uncertainties of the suggested method.

Subject headings: cosmology:theory — gamma rays:bursts — methods:data analysis

1. Introduction

Since gamma-ray bursts (GRBs) were first discovered in late 60's (Klebesadel et al. 1973), thousands of GRBs have been detected up to date. The discovery of afterglows in other spectral bands and host galaxies enabled us to measure redshifts of about twenty GRBs (see, e.g., [http : //www.aip.de/ ~ jcg/grbgen.html](http://www.aip.de/~jcg/grbgen.html)), establishing the fact that GRBs are indeed cosmological (Mao and Paczyński 1992; Meegan et al. 1992; Piran 1992; Metzger et al. 1997). Nonetheless, the redshifts are still unknown for most of the detected GRBs. Unless we locate a burst on the sky by immediate follow-up observations, the distance of the burst is apt to remain unrevealed forever.

Concerning physical models of GRBs, their distance scales are related to key issues, such as, energetics, burst rates as a function of redshifts. That is, estimating the distance puts direct constraints on the theories of the observed GRBs. Besides this the redshift distribution of GRBs should track the cosmic star formation rate of massive stars, if GRBs are indeed related to the collapse of massive stars (Woosley 1993; Paczyński 1998; MacFadyen and Woosley 1999). Therefore, once its association has been proven, one expects the observed GRBs are the most powerful probe of the high redshift universe (Wijers et al. 1998; Blain and Natarajan 2000; Lamb and Reichart 2000). In fact, the GRB formation rate and the star formation rate (SFR) have similar slopes at low redshift, implying that GRBs can be used indeed as a probe of the cosmic star formation rate at high redshift. Observations of faint galaxies have been used to estimate the history of star formation activity (Madau et al. 1996; Rowan-Robinson 1999; Steidel et al. 1999). However, there are considerable difficulties and uncertainties in the corrections that should be applied due to extinction and obscuration. An independent determination and test of the relative amount of obscured and unobscured star formation activity would be extremely valuable.

At present, there are too few redshift measurements with which to produce the global GRB formation rate. This fact is indeed hard to avoid unless observers set up networks of efficient telescopes in order for an immediate follow-up observations. Recently, however, there are pilot studies to overcome the technical ability mentioned above (e.g., Reichart et al. 2001), though there have been several attempts to quantify pulse shapes of GRBs and interpret results in terms of GRB physics (Fenimore et al. 1996; Norris et al. 1996; In'T Zand and Fenimore 1996; Kobayashi et al. 1997; Daigne and Mochkovitch 1998; Fenimore 1999; Panaitescu et al. 1999). Several authors (Stern et al. 1999; Fenimore and Ramires-Ruiz 2000; Reichart et al. 2001) began to observe strong correlations between temporal properties of the observed GRBs and their brightness, which may have some implications that the measured spikiness can be used to obtain distances much like a Cepheid-like distance estimator. Norris et al. (2000) also showed the spectral lag/luminosity relationship for six

bursts with known redshifts can be appreciated. Currently, the luminosity estimator yields best-estimate luminosity distances that are accurate to a factor of ≈ 2 (see Reichart et al. 2001).

Along the line of efforts of such kinds we propose a new method based on an empirical relation motivated by the work of Chang (2001). It is well known that power density spectra (PDSs) of long GRBs show a power-law behavior (Beloborodov et al. 1998, 2000). Though its underlying physical mechanism is not obvious (Panaiteescu et al. 1999; Chang and Yi 2000), the PDS analysis may provide useful information of physics of GRBs (Panaiteescu et al. 1999) and the distance information (Chang 2001). Particularly, Chang (2001) has demonstrated that the power-law index of PDSs of the observed GRBs shows a redshift dependence, implying a possible relationship between the power-law index and the redshift of GRBs. It can be possibly worked out because of the fact that burst profiles should be stretched in time due to cosmological time dilation by an amount proportional to the redshift, $1 + z$.

In §2 we begin with a brief summary of the PDS analysis in GRB studies, and describe the empirical relation involved in our procedure. In §3 we present results obtained by applying our method to the GRBs observed by the BATSE instrument aboard the *Compton Gamma Ray Observatory* (Paciesas et al. 1999), and discuss what they suggest. Finally, we conclude by pointing out that the accuracy of our redshift estimates is limited by unknown underlying properties of GRBs and what should be further developed in §4.

2. Empirical Relation of Power-law Index and Redshift

Contrary to the diverse and stochastic behavior in the time domain, long GRBs show a simple behavior in the frequency domain (e.g., Beloborodov et al. 1998). The power-law behavior is seen even in a single burst when it is bright and long. The power-law PDS provides a new tool for studies of GRBs themselves. Using the PDS analysis, Panaiteescu et al. (1999) analyzed the temporal behavior of GRBs in the framework of a relativistic internal shock model. They set up their internal shock model and attempted to identify the most sensitive model parameters to the observed PDS, which is defined by the square of the Fourier transform of the observed light curve. They concluded that the wind must be modulated such that collisions at large radii release more energy than those at small radii in order to reproduce consistent PDSs with the observation. However, it is also noted that the reported power-law behavior with the index of $-5/3$ and the exponential distribution of the observed PDS can be reproduced by adjusting the sampling interval in the time domain for a given decaying timescale of individual pulse in a specific form of GRB light curves (Chang

and Yi 2000). Therefore, conclusions on the central engine of GRBs on the basis of the PDS analysis should be derived with due care.

Another valuable use of the PDS analysis can be realized bearing in mind that for a given sampling interval the resulting power-law index is dependent upon the characteristic timescale of the observed light curve. For instance, consider a GRB light curve as a sum of exponential functions of time, $f(t)$, as considered in Chang and Yi (2000). Since the Fourier transform of $f(at)$ is given by $\frac{1}{|a|}F(\nu/a)$, where $F(\nu)$ is the Fourier transform of $f(t)$, ν being the cyclic frequency and a being a constant, fitting of the power law function to the PDS may result in a different power-law index as the constant a varies when the sampling interval is pre-determined. In other words, for the observed GRB light curves with the pre-determined sampling intervals, e.g., 64 ms, the cosmological time dilation stretches the light curve by an amount of $1 + z$ and consequently results in changes in the obtained power-law index. This should be true because cosmological objects like GRBs should not only be redshifted in energy but also extended in time because of the expansion of the universe. Chang (2001) demonstrated that a cosmological time dilation effect is indeed imprinted in the light curves of the observed GRBs whose redshifts are known by dividing the GRBs into near and far groups. The author has showed that the near GRB group ends up with the smaller power-law index than the far one and that the correction with the $1 + z$ factor removes the differences. The power-law index difference in two separate groups is larger than that among different energy bands.

In order to construct the empirical relation between the power-law index and the redshift of GRBs we have calculated the power-law index of the PDSs of 9 GRBs detected by the BATSE with known redshifts. We have used light curves of the GRBs from the updated BATSE 64 ms ASCII database¹. From this archive we select the light curves of the GRBs in channel 2 whose redshifts are available. We list up the GRBs used in our analysis with their reported redshifts in Table 1. We calculate the Fourier transform of each light curve of the GRBs and the corresponding PDS. Before taking the Fourier transform of light curves we scale them such that the height of their highest peak has unity in the GRB light curves. Since the individual PDS of GRBs are stochastic, different parts of the PDS appear to follow a slightly different power-law index. Having calculated the PDS of an individual GRB we obtain the power-law index of the PDS using the limited part of the PDS, i.e., $-1.6 < \log \nu < 0$. The lower bound is roughly determined in that the deviation from the power law begins due to the finite length of bursts. The upper bound is where the Poisson noise becomes dominant. Poisson noise in the measured count rate affects the PDS at high

¹ftp : //coss.gsfc.nasa.gov/pub/data/batse/

frequencies and has a flat spectrum. The Poisson noise level equals the burst total fluence including the background in the considered time window. We calculate the individual Poisson level for each burst and subtract it from the burst PDS.

The PDSs can be described as a single power law with superimposed fluctuations which follow the exponential distribution, which may require the maximum likelihood method. However, by considering that we smooth the PDSs on the scale $\Delta \log \nu = 0.5$ before fitting, the least squares fit can be preferred since the error distribution may be modified to the normal distribution according to the *central limit theorem*. We use two different fitting routines corresponding to the normal error distribution and the exponential error distribution. We employ both fitting algorithms to compare. What is shown in Figure 1 are empirical relations of the redshift and the power-law index obtained by the least squares fit and the maximum likelihood method. Firstly, we attempt to construct the empirical relation of the redshift and the power-law index without averaging of the PDSs. That is, we construct the best fit using power-law indices of 9 individual data points. Results are also shown in Figure 1, where the thin solid line results from the least squares fit, the thin dashed line the maximum likelihood method. A possible alternative way to extract the empirical relation from the noisy individual PDSs is to take the average PDSs over a sample of long GRBs. Then the random fluctuations affecting each individual PDS tend to cancel each other and the power-law behavior can be clearly seen. Because of the small number of data, we group the PDSs into 4 subgroups according to the reported redshifts, and average the PDSs before a fitting process : GRB 980329 + GRB 971214, GRB 990123 + GRB 990506 + GRB 990510, GRB 970508 + GRB 980703 + GRB 991216, GRB 980425. The thick solid line results from fitting of averaged PDSs by the least square fit, the thick dashed line the maximum likelihood method. We note that individual fitting results in a less steeper relation. We also have attempted higher order polynomial fits but it did not end up with a monotonic relation as one should expect.

The error estimates of z , which are defined by a square root of the average of squared difference between the measured redshifts summarized in Table 1 and the expected redshifts by the fitting, are 1.09 and 1.11 for the empirical relation due to individual PDS fits, 1.72 and 1.56 due to the averaged PDS fits, for the least squares fit and the maximum likelihood fit, respectively.

3. Spatial Distribution of GRBs

We adopt light curves of the long GRBs from the updated BATSE 64 ms ASCII database as in processes above. We choose bursts with durations $T_{90} > 20$ s, where T_{90} is the time it

takes to accumulate from 5 % to 90 % of the total fluence of a burst summed over all the four channels. Of those bursts, we further select bursts with the peak count rates satisfying C_{\max}/C_{\min} for the 64 ms trigger timescale is greater than 1. Applying these criteria, we end up with 388 bursts.

In a similar way, we obtain power-law indices of PDSs of the selected GRBs and subsequently estimates of their redshifts. In Figure 2, the redshift distributions of the GRBs obtained by the relation we have in the previous section are shown. Different line types indicate same meanings as in Figure 1. Note that the thin dotted histogram represents the spatial distributions of the 22 GRBs whose redshifts are available at the web site, from where the quoted redshifts in Table 1 are taken. It is interesting to note that the predicted redshift distributions of GRBs that are derived from fitting of individual power-law index without averaging PDSs appear to provide a better agreement with the redshift distribution of the GRBs with redshift-known.

The obtained GRB redshift distribution is quite suggestive. Firstly, it is seen in Figure 2 that the long GRBs observed by the BATSE, at least, are distributed well within $z \sim 5-6$. If one accepts an idea that the GRB formation rate should trace the SFR at high redshifts as at low redshifts, this is in apparent contrast to what is derived from some theoretical calculations of star formation. Theoretical calculations show that the birth rate of Pop III stars produces a peak in the SFR in the universe at redshifts $16 \lesssim z \lesssim 20$, while the birth rate of Pop II stars produces a much larger and broader peak at redshifts $2 \lesssim z \lesssim 10$ (Ostriker and Gnedin 1996). Secondly, according to the cumulative redshift distributions derived in terms of beaming-induced luminosity functions an extreme shape of a conic beam seems likely to be ruled out : although the observed $\langle V/V_{\max} \rangle$ can be satisfied with the theoretical $\langle V/V_{\max} \rangle$, a broad beam cannot explain the observed redshifts greater than $\sim 2-3$ (Kim et al. 2001) and a hollow beam expects too many GRBs farther than $z \sim 5-6$ (Chang and Yi 2001), if a SFR-motivated number density distribution of GRB sources is assumed.

4. Discussions

There are problems and limits to determine redshifts accurately in both obtaining the relation and applying this relation to data. First of all, even though this method is in principle to work, it is not clear whether we may apply this method over the observed GRB light curves obtained by various satellite missions at the same time. It is partly because the PDS of each individual burst is composed of the power law and superimposed exponentially distributed fluctuations which make it difficult to recognize the power law in an individual burst, and

partly because such the empirical relation is susceptible to observational conditions, such as, trigger timescale, detection sensitivity. Availability of more redshifts of GRBs may help to reproduce a better relation. With all the efforts in implementing a sophisticated algorithm to accommodate the diversity of the light curves, it is essential to understand a fundamental mechanism of GRBs to derive the intrinsic relation of the power-law index and the redshift. Secondly, We have implicitly assumed that all the long GRBs have a more or less same characteristic timescale and cosmological time dilation alone affects varying the characteristic timescale. We need to understand clearly what and how forms the flat part of PDS. Thirdly, the effect of redshift tends to flatten PDSs of GRBs on the contrary to the time dilation effect. It reflects a well-known fact that pulses in a single GRB are more narrow in a higher energy band (e.g., Norris et al. 1996). These effects combine and produce undesirable results in obtained power-law index. We have presumed in this study that the time dilation effect on the power-law index is larger than that of the redshift as observed in Chang (2001) and ignored the effect of the redshift. However, it should be understood how the power-law index relates with the energy channels to improve the proposed method accommodating the redshift effect.

We conclude by pointing out that, even though redshift estimates are subject to the stochastic nature of the observed PDSs and accuracy of estimates are limited by unknown properties of the GRBs the encouraging conclusion of this study is that redshifts of the GRBs can be obtained with the GRB light curves, whose redshifts otherwise remain unknown forever.

SJY is supported by the Creative Research Initiatives Program of the Korean Ministry of Science and Technology. This research has made use of data obtained through the High Energy Astrophysics Science Archive Research Center Online Service, provided by the NASA/Goddard Space Flight Center.

REFERENCES

- Blain, A. W. and Natarajan, P. 2000, MNRAS, 312, L35
- Beloborodov, A., Stern, B., and Svensson, R. 1998, ApJ, 508, L25
- Beloborodov, A., Stern, B., and Svensson, R. 2000, ApJ, 535, 158
- Chang, H.-Y. 2001, ApJ, 557, L85
- Chang, H.-Y. and Yi, I. 2001, ApJ, 554, 12
- Chang, H.-Y. and Yi, I. 2000, ApJ, 542, L17
- Daigne, F. and Mochkovitch, R. T. 1998, MNRAS, 296, 275
- Fenimore, E. 1999, ApJ, 518, 375
- Fenimore, E. E. and Ramirez-Ruiz, E. 2000, astro-ph/0004176
- Fenimore, E., Madras, C. D., and Nayakshin, S. 1996, ApJ, 473, 998
- In'T Zand, J. J. M. and Fenimore, E. 1996, ApJ, 464, 662
- Kim, C., Chang, H.-Y., and Yi, I. 2001, ApJ, 548, 532
- Klebesadel, R. W., Strong, I. B., and Olson, R. A., 1973, ApJ 182, L85
- Kobayashi, S., Piran, T., and Sari, R. 1997, ApJ, 490, 92
- Lamb, D. Q. and Reichart, D. E. 2000, ApJ, 536, 1
- MacFadyen, A. I. and Woosley, S. E., 1999, ApJ, 524, 262
- Madau, P., et al. 1996, MNRAS, 283, 1388
- Mao, S. and Paczyński, B. 1992, ApJ, 388, L45
- Meegan, C. A., et al. 1992, Nature, 355, 143
- Metzger, M. R., et al. 1997, Nature, 387, 879
- Norris, J. P., et al. 1996, ApJ, 459, 393
- Norris, J. P., Marani, G. F., and Bonnell, J. T. 2000, ApJ, 534, 248
- Ostriker, J. P. and Gnedin, N. Y. 1996, ApJ, 472, L63

- Paciesas, W. S., et al. 1999, ApJS, 122, 465
- Paczyński, B. 1998, ApJ, 494, L45
- Panaiteescu, A., Spada, M., and Mészáros, P. 1999, ApJ, 522, L105
- Piran, T. 1992, ApJ, 389, L45
- Reichart, D. E., et al. 2001, ApJ, 552, 57
- Rowan-Robinson, M. 1999, Ap&SS, 266, 291
- Steidel, C. C., et al. 1999, ApJ, 519, 1
- Stern, B., Poutanen, J., and Svensson, R. 1999, ApJ, 510, 312
- Wijers, R. A. M. J., et al. 1998, MNRAS, 294, L13
- Woosley, S. E. 1993, ApJ, 405, 273

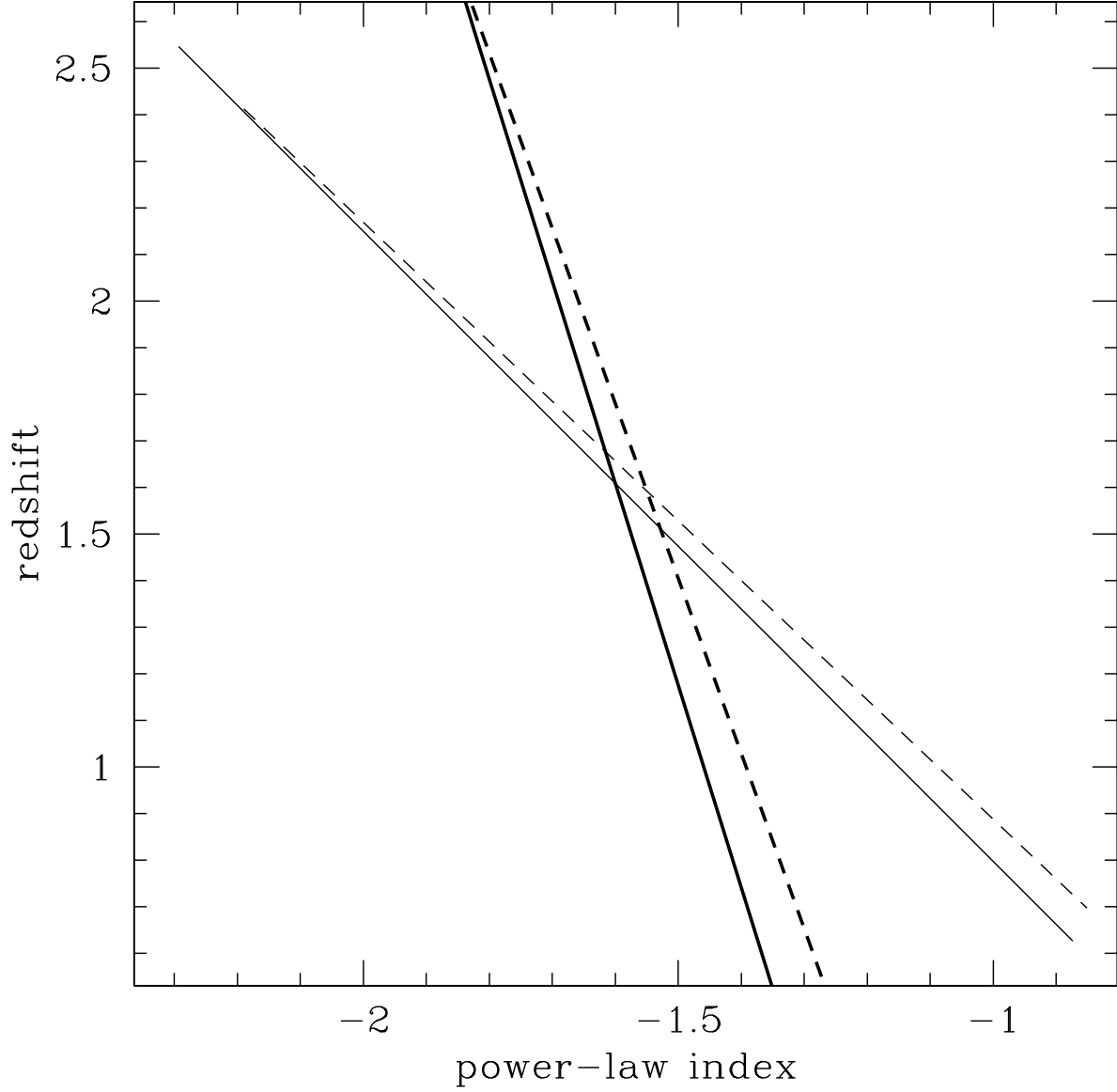


Fig. 1.— Relation of power-law index and redshift. The thin solid line results from fitting of individual PDSs by the least squares fit, the thin dashed line the maximum likelihood method. For comparison, the relation of redshift and power-law index with averaged PDSs is also shown. The thick solid line and the thick dashed line represent the least squares fit, the maximum likelihood method, respectively.

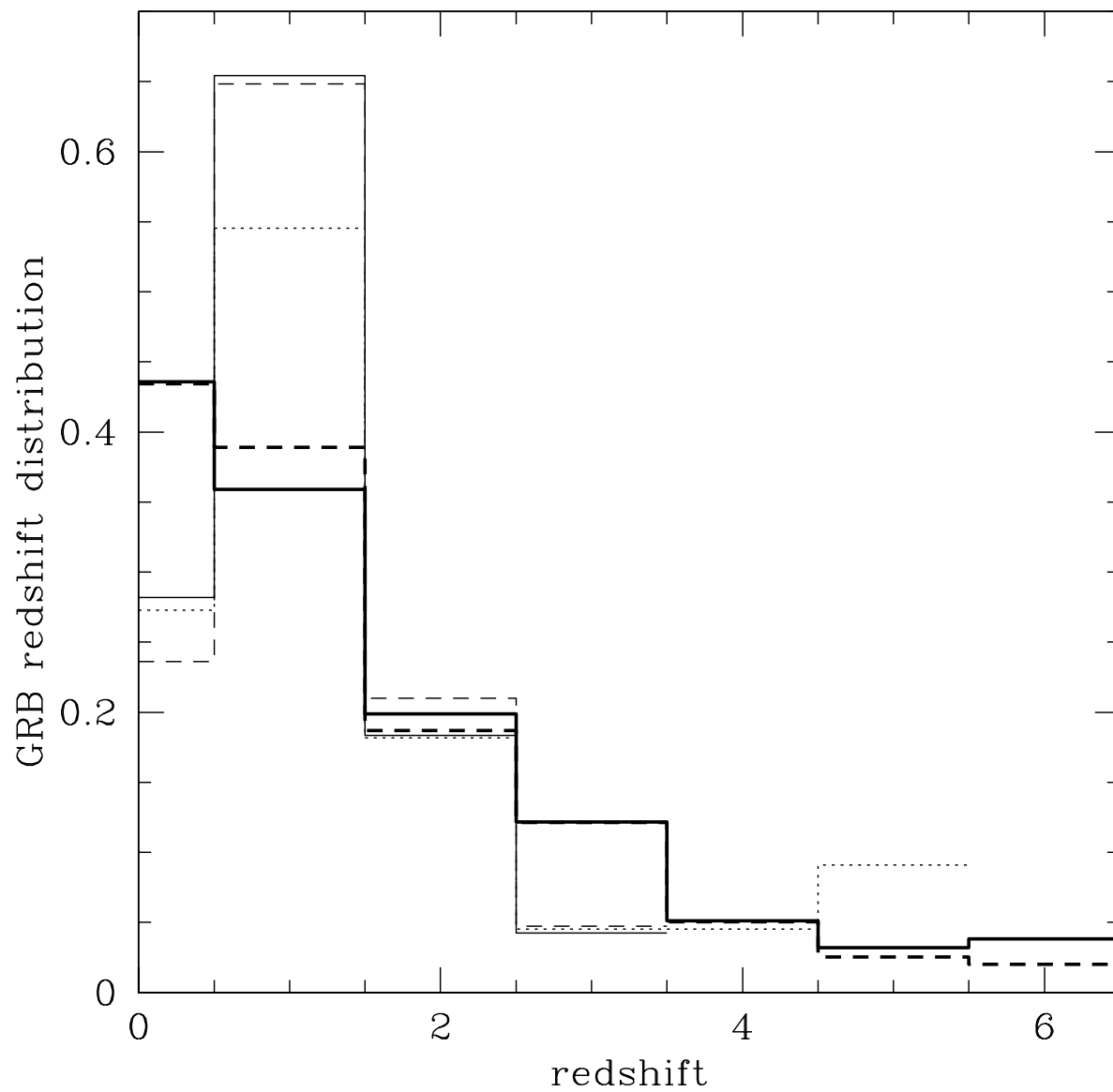


Fig. 2.— Normalized spatial distributions of 388 long GRBs observed by the BATSE are compared with that of the redshift-known GRBs, indicated by the same line types as in Figure 1 and the thin dotted line, respectively.

Table 1: A list of the GRBs used in the analysis with the redshifts and T_{90} . The redshifts are quoted from a compiled table at [http : //www.aip.de/ ~ jcg/grbgen.html](http://www.aip.de/~jcg/grbgen.html).

GRB name	trigger number	redshift	T_{90} (secs)
GRB 991216	7906	1.02	15
GRB 990510	7560	1.619	68
GRB 990506	7549	1.3	130
GRB 990123	7343	1.60	63
GRB 980703	6891	0.966	411
GRB 980425	6707	0.0085	34
GRB 980329	6665	3.9	18
GRB 971214	6533	3.42	31
GRB 970508	6225	0.835	23